DOE/ER/45310-35

DOE/ER/45310--35

DE92 004420

PROGRESS REPORT ON GRAIN BOUNDARIES

R. W. Balluffi
P. D. Bristowe

Department of Materials Science and Engineering
Massachusetts Institute of Technology
Cambridge, Massachusetts 02139

February 15, 1991 - October 15, 1991

Prepared for

U.S. Department of Energy
Under Contract DE-FG02-87ER45310

CONTENTS

1. INTRODUCTION

The present document is a progress report describing the work accomplished to date during the second year of our four-year grant (February 15, 1990 - February 14, 1994) to study grain boundaries under Grant DE-FG02-87ER45310. The research was focused on the following three major efforts:

(1) Study of the atomic structure of grain boundaries by means of x-ray diffraction, transmission electron microscopy and computer modeling

(2) Study of short-circuit diffusion along grain boundaries

(3) Development of a Thin-film Deposition/Bonding Apparatus for the manufacture of high purity bicrystals.

Efforts (1) and (2) were proposed initially for the period of the grant. Effort (3) developed out of an urgent need for an apparatus capable of producing high purity bicrystal specimens containing grain boundaries of controlled geometry. This apparatus will eventually assist us in essentially all aspects of our experimental work. Our accomplishments in each of these areas of research are described in more detail in the following. A list of all reports and publications originating from the research is presented in Section 4.

2. PERSONNEL AND GRADUATE STUDENT DEGREES AWARDED

Professor R. W. Balluffi, Principal Investigator

Dr. P. D. Bristowe, Co-Principal Investigator

Dr. I. Majid, Research Associate

Dr. A. Amiri-Hezaveh, Research Associate

Mr. C. Counterman, Graduate Student/Research Assistant (Graduated with Ph.D., 1991. Presently Post-doctoral Associate, M. I. T.)

Mr. P. Dallot, Graduate Student/Research Assistant (Graduated with Ph.D., 1991. Presently Research Scientist, Service Physique Atomique et Plasmas, France)

Mr. Qing Ma, Graduate Student/Research Assistant (Graduated with Ph.D., 1991. Presently Post-doctoral Associate, U. of Cal., Santa Barbara)

Collaborative work was also performed by:

Professor J. D. Joannopoulos (Department of Physics, M. I. T.)

Dr. M. C. Payne (Cambridge University, United Kingdom)

Mr. T. Arias, Graduate Student/Research Assistant (Department of Physics, M. I. T.)

Mr. G. P. Francis (Cambridge University, United Kingdom)

Mr. E. Tarnow, Graduate Student/Research Assistant (Department of Physics, M. I. T.)

3. RESEARCH ACCOMPLISHED

3. 1 Structural Studies

3. 1. 1. Diffraction from [111] twist boundaries in Au (1, 2)

Quantitative x-ray diffraction measurements have been made from a series of (111) gold bicrystals containing twist grain boundaries with controlled geometry. Each bicrystal was prepared at a specific angle of misorientation $\theta°$ but because of double positioning both $\theta°$ and $60\text{-}\theta°$ twist boundaries were present in the specimens. Since these pairs of boundaries have distinct structures, the intensity measurements from each bicrystal contained superimposed information representing an average from both boundary types. In order to understand these measurements in terms of the boundary structures involved, computer calculations were performed to characterize the theoretical scattering effects expected from [111] twist boundaries related by double positioning. By comparing the measurements with the calculations, it was possible to determine the conditions under which reliable structural information concerning doubly positioned twist boundaries could be obtained. From an appropriate analysis of the data, it was concluded that [111] twist boundary displacement fields are generally weak, rotational in form and centered on "O" lattice sites.

3. 1. 2. Morphological approach to constructing interatomic potentials (3)

A framework for constructing interatomic potentials is proposed and applied to the case of silicon. The construction relies on a geometrical approach in which we try to reproduce the morphology of the Born-Oppenheimer surface. In particular, we develop a new technique for constructing four body terms. It consists of building invariant coordinate systems on the configuration space of four atoms, thus allowing the choice of the four body term morphology. The potential that we develop has a two and a four body part. It is adjusted to match the only geometrical information known from the Born-Oppenheimer surface which is the position of its minimum of energy and its curvature at that point, as given by the dynamical matrix. The potential is then tested on point defects and surface structures in silicon.

3. 1. 3. Ab initio investigations of surfaces and grain boundaries in Ge (4)

In the total energy pseudopotential method calculations are performed using periodic supercells, the ionic potentials are replaced by pseudopotentials and the electronic wavefunctions are expanded in terms of a plane wave basis set. Density functional theory is used to map the system of interacting electrons onto a system of non-interacting electrons moving in an effective potential, V_{xc}, the exchange-correlation potential. The electronic groundstate is determined by solving the self-consistent Kohn-Sham equations for the electrons. The total energy of the system, the forces on the ions and the stresses on the unit cell can all be computed once the groundstate electronic configuration has been located. Since the forces on the ions can be calculated the equilibrium geometry of the system can be determined as part of the calculation.

Total energy pseudopotential calculations have been used to calculate accurate equilibrium lattice constants, bulk moduli and phase transition pressures and temperatures. The numerical methods used to locate the electronic groundstate have developed extremely rapidly in recent years following the introduction of the molecular dynamics method by Car and Parrinello. These methods allow total energy pseudopotential calculations to be applied to much larger systems than previously possible so that calculations can now be routinely performed on systems containing up to one hundred atoms in the unit cell. A conjugate gradients method has recently been developed which should allow calculations to be performed on systems containing hundreds of atoms in the unit cell. In the future with the use of parallel computers it will be possible to study systems containing a thousand atoms in the unit cell thus allowing increasingly complex systems to be investigated using the total energy pseudopotential technique.

3. 1. 4. Reduced coordinates on the configuration space of 3 and 4 atoms (5)

A framework for constructing three and four body interatomic potentials is proposed. The study is motivated by a need for an understanding of the morphology of these potentials and consequently the morphology of the Born-Oppenheimer energy surface (i.e., the location of the surface minimum and saddle points). Invariant coordinate systems on the configuration space of three and four atoms are therefore developed which allow the morphology of three and four body terms to be chosen. Direct applications of these coordinates include the construction of interatomic potentials and an analysis of the local geometry around an atom in a crystal.

3. 1. 5. Born-Oppenheimer surface of triatomic Si (6)

The Born-Oppenheimer (BO) surface of triatomic silicon is investigated and accurately described using two and three body potentials. The topology of the BO surface is found to be unstable with respect to fluctuations in these potentials, indicating that it is non generic. Examination of the two and three body components shows that the topology of the three body term is fundamentally different from that of potentials usually used to model crystalline silicon. A study was therefore made to determine under what conditions this new topology could successfully reproduce the diamond cubic structure of crystalline silicon. Two limited methods for applying these potentials in the bulk have been considered and appraised. One of them uses the exact two and three body terms, and approximates the effect of the remaining terms in the N body expansion (the screening effect) with a four body term. The other method consists of screening the two and three body terms directly. Both methods were unsuccessful in reproducing the diamond cubic structure which indicates the importance of terms of order higher than four.

3. 1. 6. Structural studies by computer simulation of grain boundary segregation (7)

The effect on observable X-ray grain boundary structure factors of the calculated segregation of solute atoms to grain boundaries is considered. Gold alloy grain boundaries are modeled using Monte Carlo simulation with embedded-atom method potentials. A range of gold-silver and gold-rich gold-nickel alloys are simulated. Pure twist $\Sigma = 5$ (θ=36.87°) [001], $\Sigma = 13$ (θ=22.62°)[001], $\Sigma = 17$ (θ=28.07°[001], and $\Sigma = 113$ (θ=7.63°)[001] grain boundaries are studied. Static relaxations of individual configurations from the Monte Carlo simulations are performed. Structure factors in the L = 0 plane and for selected relrods are calculated. Kinematical diffraction analysis is used to interpret the results. The results are compared to previous calculations and ongoing X-ray diffraction studies of these systems.

Segregation to the boundary region was observed. The segregation was much stronger in the Au-Ni alloys, where the atomic size difference was large. Clear preferences for certain sites in the boundary to be occupied by a particular component of the alloy system was found in both Au-Ag and Au-Ni systems. The coincident site in each of the Σ5, Σ17, and Σ13 boundaries was preferentially occupied by the larger atom of the

alloy; sites near grain boundary dislocations were preferentially occupied by the smaller atom. In Σ 113 boundaries segregation within the planes nearest the boundaries was for the smaller atom to the core of the grain boundary dislocations.

Atomic vibration amplitudes were greater in the region of the boundary, and were significantly higher in the planes immediately adjacent to the boundary. Within these planes, the coincident site vibration amplitude was smaller than that of the other atoms. Atomic vibration amplitudes were unexpectedly smaller for the bulk pure silver systems than the pure gold systems, with alloys having intermediate values.

Grain boundary expansion was greater in the pure Ag boundaries than in the pure Au boundaries. Au-Ag alloys had intermediate expansion values. The dilute Ni in the Au alloys had smaller expansions.

Significant changes in $|F|^2$ were found in the L = 0 plane. The ratios between the three strong boundary reflections A, B, and C [at (HKL) positions (r, r, 0), (r - s, 0, 0) and (r + s, 0, 0) respectively for $r^2 + s^2$ even, and (2r, 0, 0), (r - s, r - s, 0) and (r + s, r + s, 0) for $r^2 + s^2$ odd] vary in alloy systems, and between pure Au and pure Ag. These ratios may be used as an experimental test of these calculated structures. The shapes of relrods in each boundary change with the addition of alloying elements, only slightly in the low-angle boundaries but increasingly with increasing twist angle. The FWHM of the B relrods was found to be an indicator of boundary width. The value was larger than the dislocation spacing *d* for the highest and lowest angle boundaries studied. The FWHM indicated that the Ag systems had slightly narrower boundaries than the Au systems.

Atomic vibration amplitudes were calculated from the ratio of the averaged $|F|^2$ calculated for 100 configurations from the Monte Carlo simulations to $|F|^2$ calculated from the average positions determined from these configurations, through the Debye-Waller factor. The result from lattice reflections was slightly higher than the values computed in real space for the bulk systems; the increase is thought to be due primarily to the presence of free surfaces and the grain boundary. In both real space calculations and the Debye-Waller factor the mean displacements for the atoms in pure Au systems was found to be greater than that for the pure Ag systems; this is counter to expectations. The vibration amplitudes for

grain boundary reflections were larger than the bulk values, and generally increased with increasing twist angle. The Debye-Waller factors calculated for different grain boundary reflections at a given twist angle varied.

3. 2 Grain boundary diffusion studies (8, 9)

The effects of grain boundary structure on grain boundary diffusion in the Au/Ag system were investigated both experimentally and theoretically.

A new experimental method, called the multi-crystal surface accumulation method was developed for this study. In this method, lattice diffusion was frozen out, and during the diffusion annealing the Ag atoms diffused through thin film specimens along transverse grain boundaries from the source surface to the accumulation surface. All transverse boundaries were of the same type. This method enabled measurements of grain boundary diffusivities with a high degree of consistency at low temperatures ($T < \frac{1}{3} T_m$), and therefore made it possible, for the first time, to study structural effects in the type-C kinetics regime. The method was also capable of eliminating possible chemical effects on diffusion due to grain boundary segregation and diffusion induced grain boundary migration.

Grain boundary diffusivities were measured for a series of symmetric [001] tilt boundaries with 16 different structures including CSL boundaries of low-Σ (i.e., 5, 13, 17, 25) and more general boundaries with tilt angles between the low- Σ misorientations. The diffusivities were found to vary monotonically with tilt angle and could be rather satisfactorily fitted with a Structural Unit model description with delimiting boundaries: Σ1(100), Σ17(410), Σ5(310), Σ5(210), Σ13(320), and Σ1(110). The absence of cusps at the low-Σ misorientations suggests that the effect of the elastic field produced by the secondary dislocations on the grain boundary core structure is weak. It was also suggested that previous observations of deep cusps in $s_b\delta_b D_b$ curves at low-Σ misorientations may have been due to grain boundary segregation or DIGM effects. The temperature dependence of measured grain boundary diffusivities gave well defined activation energies of ~ 0.7 - 0.85 eV, which were smaller than the average value of ~ 1.0 eV, obtained at high temperatures in previous studies. Correspondingly, the measured pre-exponential factors (i.e., $\delta_b D^o_b$ values) were ~ 3 orders of magnitude smaller

than those obtained at high temperatures. Both Arrhenius parameters were found to be smooth functions of tilt angle.

Four representative grain boundaries: $\Sigma5(310)$, $\Sigma13(510)$, $\Sigma5(210)$, and $\Sigma13(320)$ were selected for computer simulation study. The interstitalcy mechanism was found to be of considerably lower activation energy than the vacancy mechanism in all of the 4 boundaries. The agreement in activation energy between the calculated values for the interstitialcy mechanism and the measured values was excellent for 3 of the 4 boundaries: $\Sigma5(310$, $\Sigma5(210)$, and $\Sigma13(320)$. Calculated results also indicated that the low activation energy atomic jumping paths were of the same type for the 4 boundaries and were contained within the structural units associated with the Structural Unit model.

Studies of correlated diffusional walks by computer simulation in both idealized and realistic grain boundaries revealed that there exist several possible confinements for a correlated walk, corresponding to different effective dimensionalities of the diffusion paths. By using the calculated correlation factors and simple kinetic theory, the $\delta_b D^o_b$'s were estimated for the 4 representative boundaries. Excellent agreement was found between the measured $\delta_b D^o_b$'s and the estimates with respect to both the general magnitude and the trend of the structural dependence. The results also suggested that the effective grain boundary width for grain boundary diffusion at low temperatures is close to the average interatomic distance. To explain the large difference in magnitude between the $\delta_b D^o_b$'s measured at relatively low and high temperatures, and in fact, the overall upward curvature found in the Arrhenius diagram, possible effects due to anharmonicity of atomic interaction and additional diffusion mechanisms associated with multiple boundary defects were suggested.

3.3 Construction of thin-film deposition/bonding apparatus for the manufacture of high purity bicrystals

During the last year, we have essentially completed the construction of a UHV thin-film deposition and bonding apparatus which will allow us to produce thin-films of a wide variety of metals and weld them together in situ in a single apparatus under UHV conditions without any exposure to air. The resulting specimens should be of high perfection and free of impurities, and, hence, should be ideal for further basic studies of the structure and properties of grain boundaries (and also heterophase

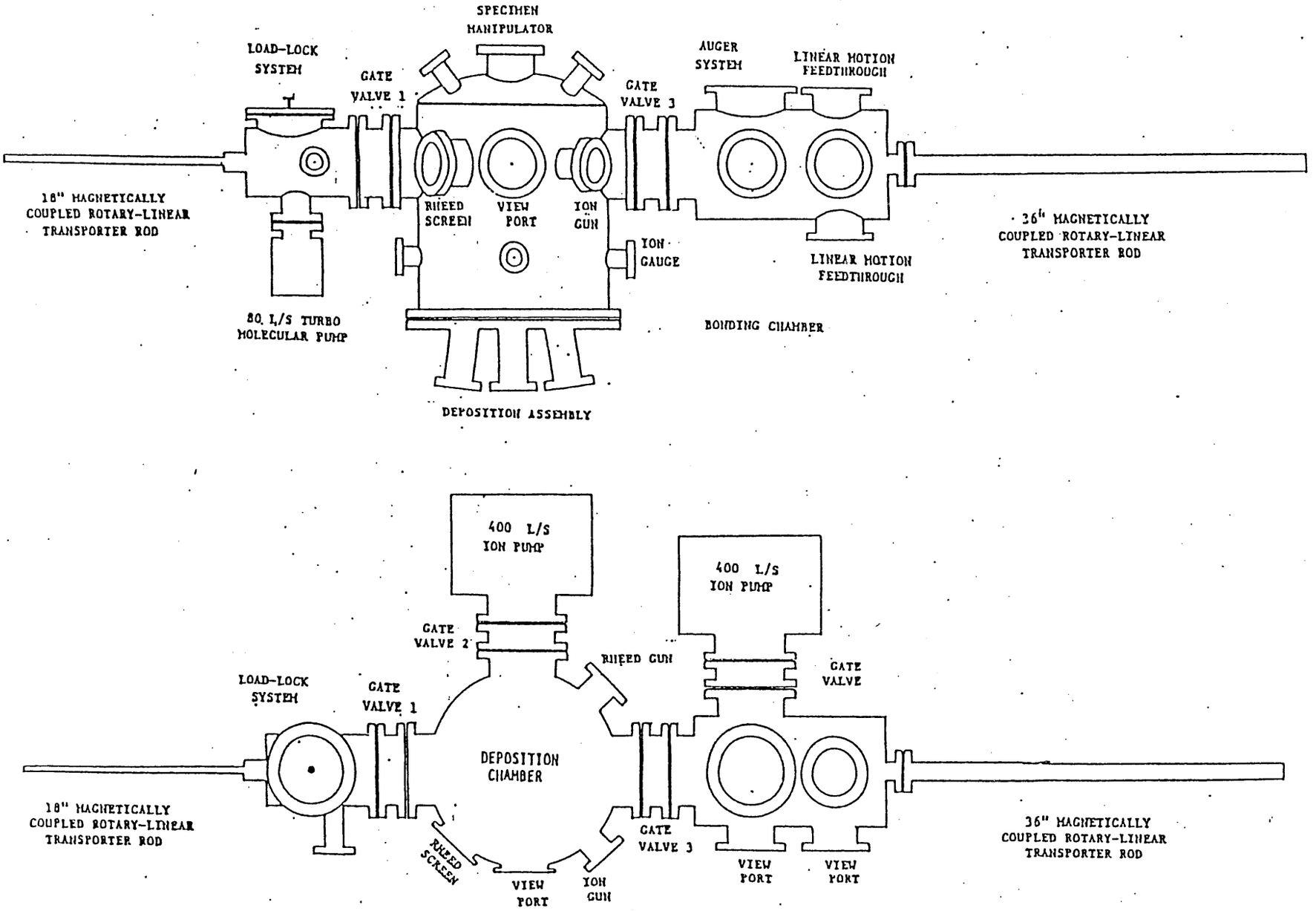
SPECIMEN MANIPULATOR
LOAD-LOCK SYSTEM
GATE VALVE 1
GATE VALVE 3
AUGER SYSTEM
LINEAR MOTION FEEDTHROUGH
18" MAGNETICALLY COUPLED ROTARY-LINEAR TRANSPORTER ROD
RHEED SCREEN
VIEW PORT
ION GUN
ION GAUGE
36" MAGNETICALLY COUPLED ROTARY-LINEAR TRANSPORTER ROD
LINEAR MOTION FEEDTHROUGH
80 L/S TURBO MOLECULAR PUMP
BONDING CHAMBER
DEPOSITION ASSEMBLY
400 L/S ION PUMP
400 L/S ION PUMP
GATE VALVE 2
RHEED GUN
GATE VALVE
LOAD-LOCK SYSTEM
GATE VALVE 1
DEPOSITION CHAMBER
18" MAGNETICALLY COUPLED ROTARY-LINEAR TRANSPORTER ROD
RHEED SCREEN
VIEW PORT
ION GUN
GATE VALVE 3
VIEW PORT
VIEW PORT
36" MAGNETICALLY COUPLED ROTARY-LINEAR TRANSPORTER ROD

Figure 1

boundaries) in a wide range of materials, including metals and semiconductors. Views of the apparatus are shown in Figure 1.

a) Fast entry load-lock system:

The load-lock system allows quick and easy loading and unloading of substrates and evaporated films in and out of the deposition chamber without breaking the UHV system. The substrate crystals are first mounted onto two holders, each have 5 sites. In order to obtain bicrystals of specified misorientations in the subsequent welding operation, one of the substrate holders has the ability to produce variable but precise rotational positioning. The substrates are then loaded onto the internal transporter through the quick access door of the specimen transfer load-lock chamber. After the specimen transfer chamber is pumped to 10^{-9} Torr by a 80 *l*/s turbo molecular pump, backed by a mechanical pump, the c-lock gate valve (1) is opened for access into the deposition chamber. The substrates are then transferred to the deposition chamber by an 18 in. magnetically coupled rotary-linear transporter rod.

b) Deposition system

The deposition system consists of a 21 in. x 18 in. UHV chamber with a liquid nitrogen shroud assembly, a UHV precision specimen manipulator, a 10 KeV Reflection High Energy Electron Diffraction (RHEED) gun, a RHEED phosphorus screen, a 2 KeV ion sputtering gun and deposition assembly. The chamber is pumped by a 400 *l*/s ion and a titanium sublimation pump with a liquid nitrogen cryo-shield.

The UHV precision specimen manipulator, with x, y, z rotary (360°) and co-axial motions, is mounted on top of the deposition chamber in order to support the specimen holders. Because of the maneuvering abilities of the manipulator, the substrates can be placed in front of the RHEED system, deposition assembly or a sputtering ion gun. Before the thin-film deposition, the substrate surfaces are sputter-cleaned by a 2 KeV ion gun. The deposition system consists of four 20 cc effusion cells which are mounted onto four 4.5 in. x 6 in. water-cooled ports, with a multiple shutter mechanism for beam selection. The whole assembly is covered by an extra liquid nitrogen shroud and then mounted at the bottom of the chamber by a 24 in. flange.

During deposition, the growth modes and crystal structure of the thin films are monitored by RHEED. The layer thickness is controlled

by observing the RHEED intensity variation (Phase Locked Epitaxy), which is a function of the atomic layer thickness during the growth.

c) The UHV bonding system

The bonding system consists of a 10 in. x 18 in. water-cooled UHV chamber, an interlock specimen transfer tube and two linear motion feedthroughs for the mounting of two specimen holders. The ports in the chamber are for Auger electron spectroscopy or Auger electron microscopy and a scanning ion sputtering gun.

The chamber is pumped through the deposition chamber with 400 l/s ion, cryo and TS pumps. In order to increase the pumping speed during the bonding operation, an extra 400 l/s ion pump is attached directly to the chamber.

After the deposition of the epitaxial thin films, the specimen holders are transferred to the UHV bonding chamber by a 36 in. long, magnetically coupled rotary-linear transport rod. The specimen holders are loaded onto two linear motion feed throughs for bonding by hot-pressing. The hot-pressing is accomplished by forcing the thin-film crystals together face-to-face by means of rods running through the linear motion feedthrough ports. during this operation, the specimen holders (and the specimens themselves) are heated resistively to the desired welding temperature.

At the present time, the apparatus has been fully assembled and vacuum tested. All of the auxiliary equipment has been installed and tested. Also, the specimen transfer mechanisms are fully operational. The evaporation sources have been charged with Al, Ni, Ag, and Si; and we are essentially in position to make our first deposition tests.

4. LIST OF ALL REPORTS AND PUBLICATIONS ORIGINATING FROM THE RESEARCH

(1) I. Majid, D. Wang and P. D. Bristowe, "Diffraction effects from [111] twist boundaries in gold", Mat. Res. Soc. Proc. 209, 47, (1991): DOE/ER/45310-28.

(2) P. Dallot and P. D. Bristowe, "A morphological approach to constructing interatomic potentials: an application to silicon", Mat. Res. Soc. Proc. 209, 159, (1991): DOE/ER/45310-29.

(3) M. C. Payne, G. P. Francis, M. Needels, E. Tarnow, P. Dallot, P. D. Bristowe and J. D. Joannopoulos, "Ab initio investigations of surfaces and grain boundaries in germanium", Springer Series in Materials Science, 17, (1991): DOE/ER/45310-31.

(4) Qing Ma and R. W. Balluffi, "Effect of grain boundary structure on grain boundary diffusivities in the Au/Ag system," Mat. Res. Soc. Proc. 209, 33, (1991): DOE/ER/45310-32.

(5) P. Dallot, P. D. Bristowe and M. Demazure, "Reduced coordinates on the configuration space of three and four atoms", Phys. Rev. B, submitted: DOE/ER/45310-33.

(6) P. Dallot and P. D. Bristowe, "Born-Oppenheimer surface of triatomic silicon and its relationship to potentials in the bulk," Phys. Rev. B, submitted: DOE/ER/45310-34.

(7) I. Majid and P. D. Bristowe, "An X-ray diffraction and computer simulation study of [111] twist boundaries in gold", Phil. Mag. A, submitted: DOE/ER/45310-36.

(8) R. W. Balluffi and P. D. Bristowe, "Progress Report on Grain Boundaries," DOE/ER/45310-35.

REFERENCES

(1) I. Majid, D. Wang and P. D. Bristowe, "Diffraction effects from [111] twist boundaries in gold", Mat. Res. Soc. Proc. 209, 47, (1991): DOE/ER/45310-28.

(2) I. Majid and P. D. Bristowe, "An X-ray diffraction and computer simulation study of [111] twist boundaries in gold", Phil. Mag. A, submitted: DOE/ER/45310-36.

(3) P. Dallot and P. D. Bristowe, "A morphological approach to constructing interatomic potentials: an application to silicon", Mat. Res. Soc. Proc. 209, 159, (1991): DOE/ER/45310-29.

(4) M. C. Payne, G. P. Francis, M. Needels, E. Tarnow, P. Dallot, P. D. Bristowe and J. D. Joannopoulos, "Ab initio investigations of surfaces and grain boundaries in germanium", Springer Series in Materials Science, 17, (1991): DOE/ER/45310-31.

(5) P. Dallot, P. D. Bristowe and M. Demazure, "Reduced coordinates on the configuration space of three and four atoms", Phys. Rev. B, submitted: DOE/ER/45310-33.

(6) P. Dallot and P. D. Bristowe, "Born-Oppenheimer surface of triatomic silicon and its relationship to potentials in the bulk," Phys. Rev. B, submitted: DOE/ER/45310-34.

(7) C. A. Counterman, "Calculations of the effects of solute segregation on grain boundary structure and X-ray structure factors in g.l.c. alloys," Ph.D. Thesis, M.I.T., June 1991.

(8) Qing Ma and R. W. Balluffi, "Effect of grain boundary structure on grain boundary diffusivities in the Au/Ag system," Mat. Res. Soc. Proc. 209, 33, (1991): DOE/ER/45310-32.

(9) Qing Ma, "Effects of grain boundary structure on diffusion along [001] tilt boundaries in the Au/Ag system," Ph.D. Thesis, M.I.T., June 1991.

END

DATE FILMED

01/23/92